EXOSKELETONS

Assistance magnitude versus metabolic cost reductions for a tethered multiarticular soft exosuit

B. T. Quinlivan,[1,2]* S. Lee,[1,2]* P. Malcolm,[1,2] D. M. Rossi,[1,2,3] M. Grimmer,[4] C. Siviy,[1,2] N. Karavas,[1,2] D. Wagner,[1,2] A. Asbeck,[5] I. Galiana,[1,2] C. J. Walsh[1,2]†

When defining requirements for any wearable robot for walking assistance, it is important to maximize the user's metabolic benefit resulting from the exosuit assistance while limiting the metabolic penalty of carrying the system's mass. Thus, the aim of this study was to isolate and characterize the relationship between assistance magnitude and the metabolic cost of walking while also examining changes to the wearer's underlying gait mechanics. The study was performed with a tethered multiarticular soft exosuit during normal walking, where assistance was directly applied at the ankle joint and indirectly at the hip due to a textile architecture. The exosuit controller was designed such that the delivered torque profile at the ankle joint approximated that of the biological torque during normal walking. Seven participants walked on a treadmill at 1.5 meters per second under one unpowered and four powered conditions, where the peak moment applied at the ankle joint was varied from about 10 to 38% of biological ankle moment (equivalent to an applied force of 18.7 to 75.0% of body weight). Results showed that, with increasing exosuit assistance, net metabolic rate continually decreased within the tested range. When maximum assistance was applied, the metabolic rate of walking was reduced by 22.83 ± 3.17% relative to the powered-off condition (mean ± SEM).

INTRODUCTION

Humans naturally walk in a manner that conserves energy; we optimize our cadence, step length, and arm swing to minimize metabolic energy consumption (*1*, *2*). It is a commonly held belief that deviations from this normal walking pattern increase energy expenditure (*3*, *4*). Certain diseases that affect gait, such as stroke, Parkinson's disease, and cerebral palsy, increase the net energy expenditure of walking by as much as 70% compared with healthy individuals (*5*–*7*). In addition, the energy expenditure of healthy individuals increases under strenuous activities, such as walking uphill or carrying heavy loads (*8*, *9*). Such increases in metabolic consumption could lead to greater levels of fatigue and injury. For patient populations, the added effort could also decrease community involvement.

Over the past decade, a number of wearable robotic devices have been developed to assist human walking and reduce metabolic energy consumption. Some of these devices comprise rigid linkages that span the entire lower limb and apply assistive torques to offset net muscle-tendon moments about the wearer's joints; however, such designs were found to increase energy expenditure, because they restricted natural gait dynamics and added large distal inertias to limb segments (*10*, *11*). Moreover, if misaligned, the rigid frames could apply undesired forces to the wearer's biological joints, further disrupting natural gait biomechanics (*12*).

Recently, several groups have tried to address these issues by using lightweight components to anchor to the body and deliver assistance to a single joint in parallel with musculature (*13*–*17*). These systems were shown to substantially reduce the metabolic cost of walking. Koller *et al.* published the highest metabolic reduction with tethered system (a 17.8% reduction relative to unpowered walking) while using a tethered pneumatic ankle exoskeleton and adaptive gain controller (*16*). The highest reduction with an autonomous system was reported by Mooney and Herr (an 11% reduction relative to walking without the exoskeleton) (*17*).

The approach of our laboratory has been to use functional apparel to comfortably and securely anchor to the human body to create soft exosuits (*18*–*20*) that can apply joint moments via tensile forces across joints in parallel with the muscles to reduce the required muscular activation. They are particularly suitable for assisting locomotion because they have extremely low distal inertia, are nonrestrictive, and create moments intrinsically aligned with the biological joints. Forces are transmitted across the body through load paths determined by the textile architecture, which are designed to provide assistance with specific motions while not interfering with others.
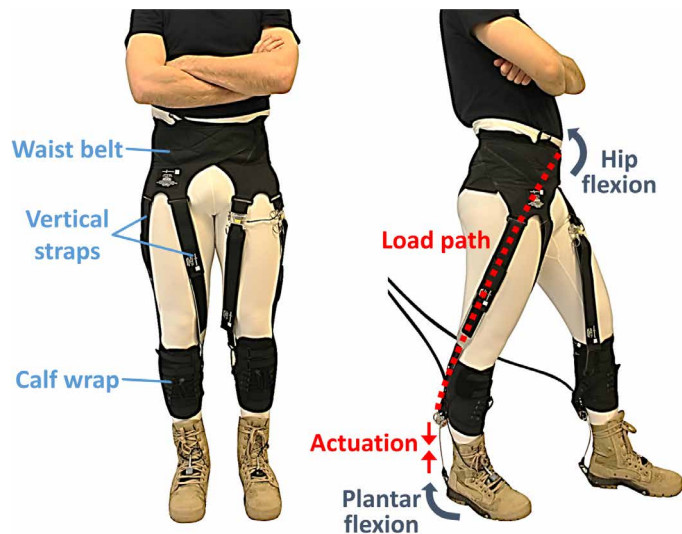
The version of the exosuit used in this study has been designed to assist with both plantar flexion and hip flexion (*21*). In brief, its textile architecture consisted of a waist belt, two calf wraps, and four vertical straps, as shown in Fig. 1. Force is applied locally to the ankle by a single actuator to provide ankle plantar flexion assistive moments, and some of this force is transmitted through the textile architecture to also provide assistive moments for hip flexion (fig. S7); the load path routes approximately through the center of the knee joint axis to minimize applied moments at the knee. Promising metabolic reductions have been previously shown for loaded walking with this multiarticular exosuit (*21*), but its efficacy on unloaded walking has yet to be evaluated.

Furthermore, when defining requirements for any wearable robot to reduce energy expenditure, including soft exosuits, it is important to maximize the user's metabolic benefit resulting from the exosuit assistance while also limiting the metabolic penalty of carrying the system's mass. Thus, trade-offs must be considered because increasing exosuit assistance requires larger motors and batteries, increasing the actuation unit mass. Consequently, the aim of this study was to

Fig. 1. Soft exosuit. The soft exosuit used in the study consists of a waist belt, two calf wraps, and four vertical straps. An actuator is used to retract the inner cable of a Bowden cable assembly and to apply a force local to the ankle to assist with plantar flexion. Some of this force is also transmitted through the vertical straps to the front of the waist belt to assist with hip flexion.

isolate and characterize the relationship between the exosuit assistance magnitude (i.e., peak exosuit ankle moment) and the metabolic cost of unloaded walking, with an understanding that the underlying mechanics of human locomotion may be used to understand changes in metabolic cost. We hypothesized that, with increasing exosuit assistance magnitude, the metabolic cost of walking would continually decrease up to a limit where it would begin to level off, as found in previous prosthesis and exoskeleton studies (*22*, *23*).

Here, we performed a series of experiments in which exosuit assistance was varied over a wide range; peak assistive force applied to the textile architecture, local to the ankle, was scaled on the basis of each participant's body weight: 18.7% (LOW), 37.5% (MED), 56.2% (HIGH), and 75.0% (MAX). While the participants walked on a treadmill, assistance was provided with an off-board actuation system to isolate the relationship between assistance and metabolic reduction, without the effect of system mass. In an attempt to deliver an assistive moment profile similar to the biological moment, we used a biologically inspired controller based on both the human kinematics and exosuit stiffness, as further described in Materials and Methods. In brief, this controller differs from those used in previous exosuit studies because the Bowden cable is retracted at a constant speed from heel strike up until the end of stance phase, gradually loading the suit throughout stance. During all trials, exosuit system data, joint kinematic and kinetic data, and metabolic rate by means of indirect calorimetry were recorded. Then, we statistically evaluated the effect of exosuit assistance across conditions.

RESULTS
Metabolic rate
As shown in Fig. 2, with increasing exosuit assistance (defined as peak exosuit ankle moment), net metabolic rate continually decreased in the tested range. A first-order analysis of variance (ANOVA) test showed that the relationship between the peak exosuit ankle moment and the net metabolic reduction fits well to a linear model [$n = 7$;
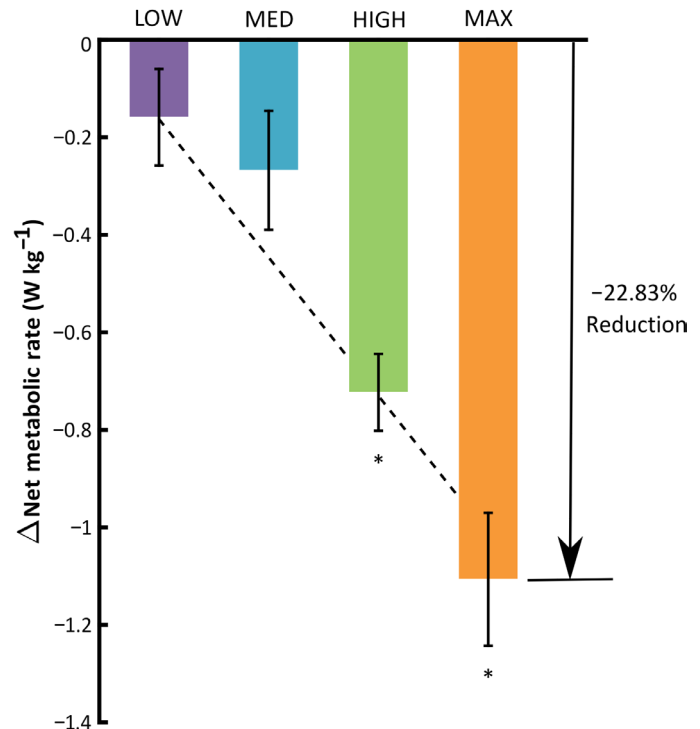
Fig. 2. Changes in net metabolic rate. Changes in net metabolic rate of the four active conditions continually decreased with increasing exosuit assistance relative to the powered-off condition. Change in net metabolic rate was -1.017 ± 0.137 W kg^{-1} (mean ± SEM) under the MAX condition, which corresponds to a 22.83 ± 3.17% decrease compared with the powered-off condition. Asterisks indicate significant differences relative to the powered-off condition (paired *t* test; $P_{HIGH} = 9 \times 10^{-5}$; $P_{MAX} = 2 \times 10^{-4}$).

ANOVA with first-order model; $y = -1.5803x + 0.1167$; y (W kg^{-1}), x (N·m kg^{-1}); $R^2 = 0.7504$, $P = 8 \times 10^{-11}$]. Under the MAX condition, the metabolic rate of walking was reduced by 1.017 ± 0.137 W kg^{-1} (mean ± SEM; paired *t* test, $P = 2 \times 10^{-4}$) relative to the powered-off condition, which is a reduction of 22.83 ± 3.17%. The average net metabolic reductions for the LOW, MED, and HIGH conditions were 3.59 ± 5.66%, 6.45 ± 5.73%, and 14.79 ± 3.62%, respectively. Changes in net metabolic rate for each participant can be found in table S1.

Kinetics
Across the four active conditions, the average peak assistive moments at the hip and ankle, respectively, were 0.201 ± 0.040 N·m kg^{-1} and 0.181 ± 0.010 N·m kg^{-1} (LOW), 0.302 ± 0.073 N·m kg^{-1} and 0.357 ± 0.016 N·m kg^{-1} (MED), 0.393 ± 0.095 N·m kg^{-1} and 0.540 ± 0.031 N·m kg^{-1} (HIGH), and 0.468 ± 0.085 N·m kg^{-1} and 0.707 ± 0.053 N·m kg^{-1} (MAX).

Ankle
With increasing exosuit assistance, peak total ankle moment during push-off, estimated using inverse dynamics, decreased ($P = 4 \times 10^{-9}$), as shown in Fig. 3. Peak biological (total minus exosuit) ankle moment during push-off also decreased ($P = 3 \times 10^{-24}$) with increasing exosuit assistance. Both average positive exosuit ankle power ($P = 2 \times 10^{-19}$) and average negative exosuit ankle power ($P = 7 \times 10^{-3}$) increased in magnitude. Average positive total ankle power increased in magnitude ($P = 4 \times 10^{-8}$) and average negative total power decreased in magnitude
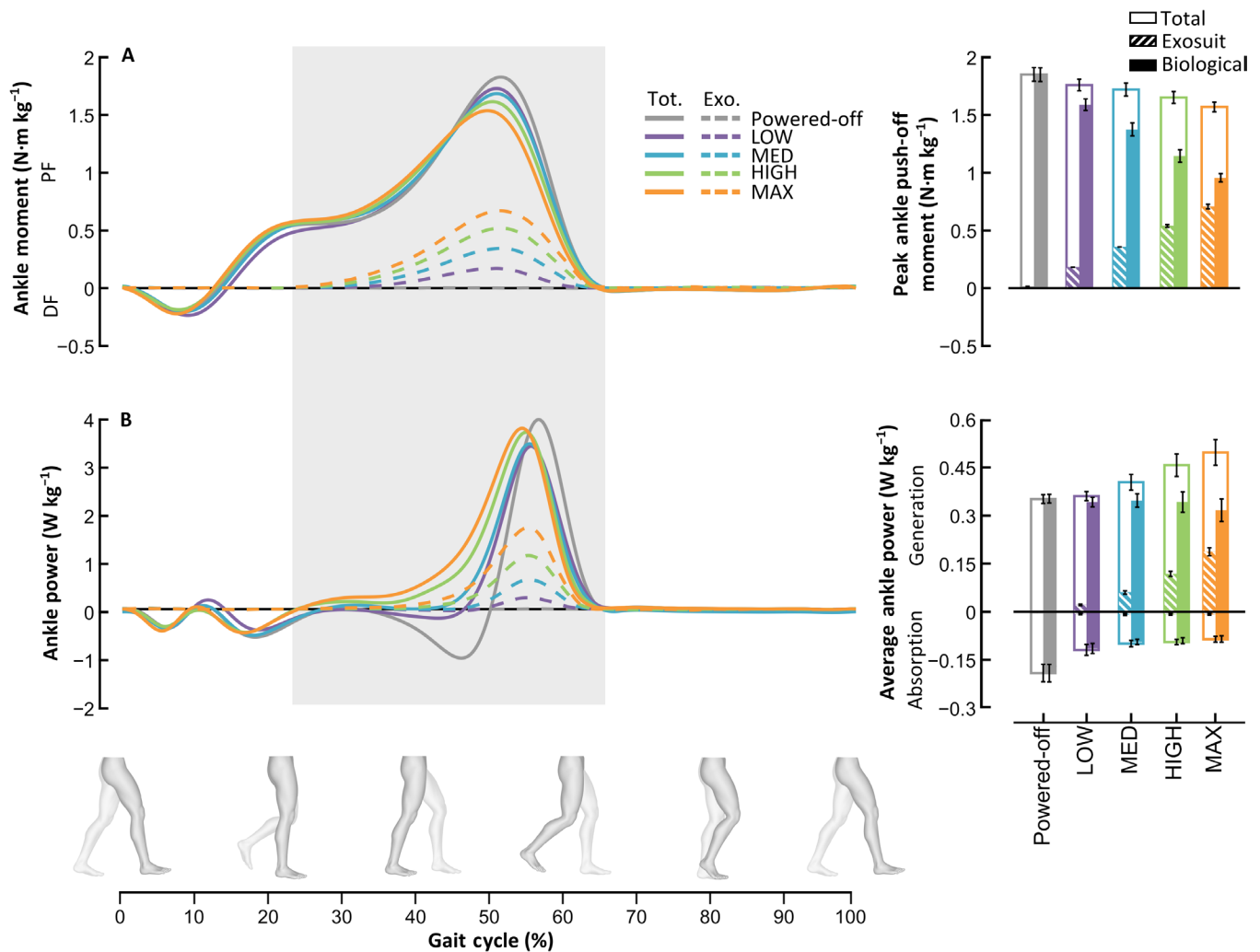
Fig. 3. Changes in ankle moment and power. (A) Total (solid line) and exosuit (dashed line) ankle moment normalized to body mass over the gait cycle for each condition, averaged across participants. Gray shading outlines approximate region during which assistance was applied. Bar graph on the right indicates the total (solid bar) and exosuit (striped bar) peak ankle moment. $n = 7$; error bar indicates SEM. ANOVA tests were run for an effect on exosuit assistance (defined as peak exosuit ankle moment). Peak total ankle moment decreased ($P = 4 \times 10^{-9}$) with increasing exosuit assistance. Peak biological (total minus exosuit) ankle moment also decreased ($P = 3 \times 10^{-24}$) with increasing exosuit assistance. **(B)** Total and exosuit ankle power. Bar graph indicates total (white bar), exosuit (striped bar), and biological (solid bar) average positive ankle power and average negative ankle power. Average positive total power increased in magnitude ($P = 4 \times 10^{-8}$) and average negative total power decreased in magnitude ($P = 4 \times 10^{-6}$) with increasing exosuit assistance. Both average positive ($P = 2 \times 10^{-19}$) and negative ($P = 7 \times 10^{-3}$) exosuit ankle power increased in magnitude with increasing exosuit assistance. Average negative biological (total minus exosuit) ankle power decreased in magnitude ($P = 7 \times 10^{-6}$) with increasing exosuit assistance. Average positive biological ankle power decreased but not significantly ($P = 0.099$). PF, plantar flexion; DF, dorsiflexion; Tot., total; Exo., exosuit.

($P = 4 \times 10^{-6}$) across conditions. Average negative biological (total minus exosuit) ankle power decreased in magnitude ($P = 7 \times 10^{-6}$) with increasing exosuit assistance. Average positive biological ankle power remained unchanged ($P = 0.099$). Average net biological ankle power increased ($P = 0.006$) with increasing exosuit assistance (fig. S10).
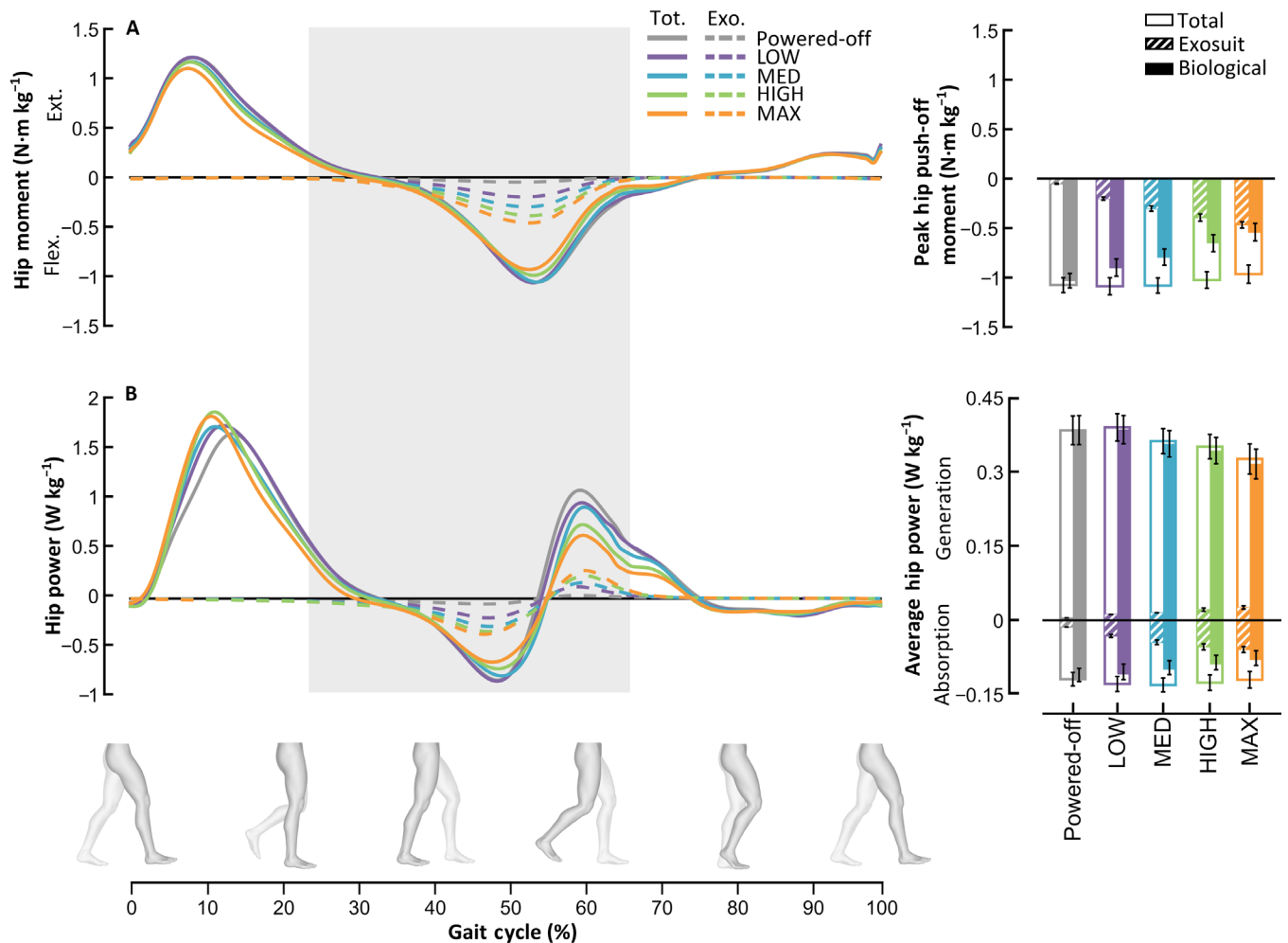
Hip
Similarly, with increasing exosuit assistance, peak exosuit hip moment during push-off increased ($P = 9 \times 10^{-19}$) and peak total hip moment during push-off decreased ($P = 3 \times 10^{-4}$), as shown in Fig. 4. Peak biological hip moment during push-off also decreased ($P = 1 \times 10^{-17}$) across conditions. Both average positive ($P = 7 \times 10^{-11}$) and negative ($P = 2 \times 10^{-13}$) exosuit hip power increased in magnitude

with increasing exosuit assistance. Average positive total hip power decreased ($P = 7 \times 10^{-6}$), whereas negative total hip power remained unchanged ($P = 0.985$). Both average positive ($P = 2 \times 10^{-7}$) and negative ($P = 3 \times 10^{-9}$) biological hip power decreased in magnitude with increasing exosuit assistance. Average net biological hip power decreased ($P = 0.004$) with increasing exosuit assistance (fig. S10).

Kinematics
As exosuit assistance increased, maximum dorsiflexion decreased ($P = 7 \times 10^{-9}$) and maximum plantar flexion increased ($P = 3 \times 10^{-10}$), as shown in Fig. 5. Maximum dorsiflexion decreased from $9.86 \pm 0.91°$ under the powered-off condition to $2.61 \pm 0.92°$ under the MAX condition (mean ± SEM). Maximum plantar flexion increased from

Fig. 4. Changes in hip moment and power. (**A**) Total (solid line) and exosuit (dashed line) hip moment normalized to body mass over the gait cycle for each condition, averaged across participants. Gray shading outlines approximate region during which assistance was applied. Bar graph on the right indicates the total (solid bar) and exosuit (striped bar) peak hip moment. $n = 7$; error bar indicates SEM. ANOVA tests were run for an effect on exosuit assistance (defined as peak exosuit ankle moment). Peak total hip moment decreased ($P = 3 \times 10^{-4}$) and peak exosuit hip moment increased ($P = 9 \times 10^{-19}$) with increasing exosuit assistance. Peak biological hip moment during push-off decreased ($P = 1 \times 10^{-17}$) with increasing exosuit assistance. (**B**) Total and exosuit hip power. Bar graph indicates total (white bar), exosuit (striped bar), and biological (solid bar) average positive hip power and average negative hip power. Both average positive ($P = 7 \times 10^{-11}$) and negative ($P = 2 \times 10^{-13}$) exosuit hip power increased with increasing exosuit assistance. Average positive total hip power decreased ($P = 7 \times 10^{-6}$), whereas negative total hip power remained unchanged ($P = 0.985$). Average positive ($P = 2 \times 10^{-7}$) and negative ($P = 3 \times 10^{-9}$) biological hip power decreased in magnitude with increasing exosuit assistance. Ext., extension; Flex., flexion.

$16.44 \pm 0.69°$ under the powered-off condition to $25.67 \pm 0.54°$ under the MAX condition (mean $\pm$ SEM). At the knee, no changes in maximum flexion or maximum extension were observed. At the hip, both maximum hip flexion increased ($P = 0.026$) and maximum hip extension decreased ($P = 5 \times 10^{-9}$) with increasing exosuit assistance.

DISCUSSION
With increasing exosuit assistance, the net metabolic rate of walking continually decreased within the tested range. Under the MAX condition, the metabolic rate of walking was reduced by $22.83 \pm 3.17\%$ relative to the powered-off condition. At the time of this submission, this is the highest relative reduction reported with a tethered exoskeleton or exosuit.

The fact that we did not see diminishing returns of metabolic reduction with increasing assistance differs from other parameter sweep studies with ankle assistive devices (exoskeletons and prostheses), which found either a leveling off or increase in metabolic rate (*13, 14, 22, 23*). Of these sweep studies, the most similar one was conducted by Jackson and Collins using a unilateral exoskeleton (*23*). In their study, metabolic rate decreased as net exoskeleton work rate at the ankle increased up to about 0.19 W kg^{-1} but remained similar after that. In our study, net exoskeleton work rate was increased up to 0.19 W kg^{-1} at both ankles, with higher values not being achievable because of limitations in the actuation system used. Thus, it is currently unknown how further increasing the exosuit assistance would result in further decreases in metabolic rate. Furthermore, it can be expected that results from such studies may differ when assistance is applied bilaterally versus unilaterally as well as
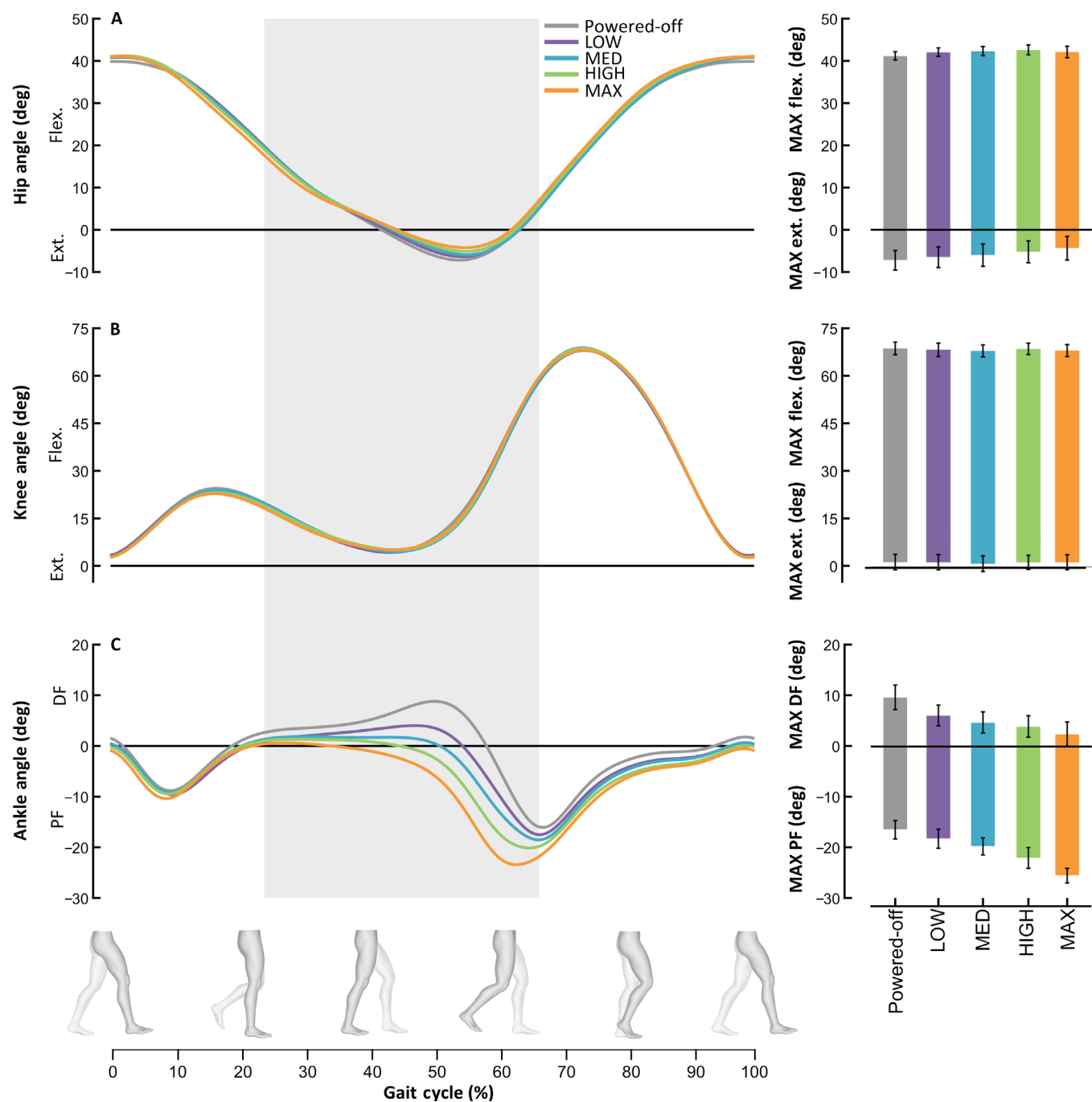
Fig. 5. Changes in joint kinematics. Left: The sagittal plane joint angle for the hip, knee, and ankle over the gait cycle averaged across all participants for each experimental condition. Gray shading outlines approximate region during which assistance was applied. Right: The peak flexion and extension angles of each joint. $n = 7$; error bar indicates SEM. ANOVA tests were run for an effect on exosuit assistance (defined as peak exosuit ankle moment). (**A**) Maximum hip extension decreased ($P = 5 \times 10^{-9}$) and maximum hip flexion increased ($P = 0.026$) with increasing exosuit assistance. (**B**) Knee flexion ($P = 0.380$) and extension ($P = 0.779$) remained unchanged. (**C**) Dorsiflexion decreased ($P = 7 \times 10^{-9}$) and plantar flexion increased ($P = 3 \times 10^{-10}$) with increasing exosuit assistance.

with different hardware and control approaches, and thus, further exploration is required to understand the effects of increased assistance with the exosuit.

A possible insight into the large metabolic reduction found in our study may be the fact that we observed significant decreases in biological moments and powers at the target joints [Figs. 3 and 4 (bar graphs) and figs. S8 and S9 (time-series graphs)]. Both the ankle and

hip biological (total minus exosuit) moments significantly decreased in magnitude as exosuit assistance increased. Similarly, positive biological power generation decreased significantly at the hip as exosuit assistance increased and biological power generation at the ankle decreased, but not significantly.

The reduction in hip power is likely a combined result of (i) direct assistance by the exosuit due to its multiarticular nature and (ii) energy

transfer between the hip and other joints as was reported in other studies (*16, 17, 24*). Unlike most other exoskeletons, which directly target only ankle plantar flexion, the multiarticular load path also transmits force to the hip joint, assisting hip flexion during late stance and early swing. Under the MAX condition, we calculated that 43.5% of peak hip flexion moment and 6.7% of hip positive work were assisted by the exosuit relative to the powered-off condition. Independent of the ankle assistance, this amount of hip assistance is already considerable compared with previous studies on hip exoskeletons showing metabolic reductions (*25*).

In addition, several studies support point (ii), the hypothesis that energy is transferred between the hip and the ankle, reducing the moment and power requirements of the hip. Koller *et al.* (*16*) and Mooney and Herr (*17*) both found significant decreases in biological hip moment and power while assisting with ankle-only exoskeletons. In addition, another study by Lewis and Ferris (*24*) that did not involve an exoskeleton found a decrease in hip moment and power while participants intentionally walked with increased ankle push-off. These results suggest that increased plantar flexion power at the ankle (either voluntary or from external assistance) during push-off can be transferred through the lower limb linkage and thus may reduce hip flexion power requirements. The current embodiment of the suit, including coupling of the hip and ankle via the multiarticular straps, may further facilitate the energy transfer between joints, potentially making locomotion more efficient. This echoes recommendations from a simulation study on exotendons, suggesting that having tendons span multiple joints and crossing from the posterior to the anterior side of the leg may be energetically beneficial for human walking (*26*). We thus hypothesize that a combined effect of (i) and (ii) is likely and that the multiarticular nature of the exosuit may have added to the effects of energy transfer with the ankle.

At the ankle, on the other hand, we observed that the overall joint kinematics and kinetics changed significantly in magnitude and timing. In particular, with increasing exosuit assistance, the negative biological power absorption during mid-stance significantly decreased, and the onset timing of the positive power phase started earlier (fig. S9C). Under the higher assistance conditions, the negative power phase was entirely removed, and the duration of positive power generation markedly increased. This differs from a previous loaded walking study from our group at the same walking speed using the same exosuit components but a different controller, which delivered assistance primarily during push-off (*21*). In this previous study, we observed a biological ankle power more similar to that of normal walking because it included a negative power region during mid-stance. This is similar to what was found in other exoskeleton studies where assistance was delivered primarily during push-off, which showed substantial metabolic benefit, including Koller *et al.* (*16*), Mooney and Herr (*17*), and Malcolm *et al.* (*14*). Thus, the results from this study motivate further studies that compare the effects of different control approaches at the ankle, in particular assistance strategies that deliver assistance during the push-off period and also earlier in stance such that the duration of the positive power phase may be increased.

However, the high metabolic reduction found in this study and an increase in the duration of positive power phase do not necessarily imply that such ankle joint behavior is energetically more efficient; rather, this may imply that, when provided with external assistance from a wearable robot, people alter their gait to maximize the benefit they receive, perhaps in an attempt to optimize their walking energetics, as proposed previously by Selinger *et al.* (*27*).

For example, in unassisted walking, the removal of the negative power absorption phase during mid-stance may be energetically detrimental because it would prevent the Achilles tendon from storing energy during stance phase to be released during push-off (*28, 29*). However, with external plantar flexion assistance, it may be more optimal to have an increased positive power phase at the ankle where a wearer can acquire more positive work directly from the exosuit. Further studies are required to understand such a trade-off.

Although this study demonstrates a high metabolic reduction when comparing an exosuit powered versus unpowered, we acknowledge that there are a number of limitations to this work. First, the precise mechanism for this high metabolic reduction remains somewhat unclear. For example, it is currently unknown whether the assistance of the hip or ankle contributed more to the metabolic reduction and how the coupling of the two via the multiarticular straps contributed to the reduction. As a result, subsequent studies focused on providing assistance separately to the hip and ankle as well as with and without multiarticular straps could help better separate the impact of both joints as well as the impact of direct assistance and energy transfer between joints. In addition, subsequent studies that focused on better understanding the underlying muscle-tendon dynamics could provide further insight into contributions to metabolic reduction. Potential studies include exosuit experiments with electromyographic measurements or muscle-level imaging techniques (*30*), as well as musculoskeletal modeling and simulation work based on experimental data (*31–33*).

Furthermore, our ability to identify the complete relationship between exosuit assistance and metabolic rate was limited by the actuation system used. With increasing assistance, the metabolic rate continually decreased without diminishing returns within the tested range, but without further increasing assistance, the maximum potential metabolic reduction achievable with this exosuit architecture and control approach is currently unknown. Additional studies that sweep to higher magnitudes of assistance are required to determine whether the descending trend in metabolic rate continues.

Another limitation of the present study is that the baseline condition for comparison was a powered-off condition and not a no-suit condition. We chose to use a powered-off condition as opposed to a no-suit condition to reduce the length of testing sessions and to avoid repositioning the markers used for kinematic analysis, which could have led to increased variability in the kinematic and kinetic results. For the version of the exosuit used in this study, we have estimated an increase in metabolic cost in the range of 2.5 to 6.5% due to the weight of the textile, sensor, and attachment components compared with walking without the exosuit. Details are included in the Supplementary Materials.

Last, because the ultimate goal with such a system is to reduce the metabolic cost of walking, further studies are required with autonomous, body-worn systems. On the basis of the actuation parameters used in this study under the MAX condition (i.e., motor torque and speed), and knowing the mass of the suit components used in this study, a conservative total system mass estimate for an autonomous system is about 6 kg (*19, 20, 34*). This estimate is made up of ~4.9 kg for actuation and batteries worn around the waist, and suit components (textile, sensors, and attachments) distributed on the trunk, both shanks, and both feet of 0.443, 0.356, and 0.364 kg, respectively.

Here, we performed a series of experiments in which the magnitude of assistance applied by a multiarticular exosuit was varied over a wide range. We found that with increasing exosuit assistance, the net metabolic rate of walking continually decreased, up to 23% compared
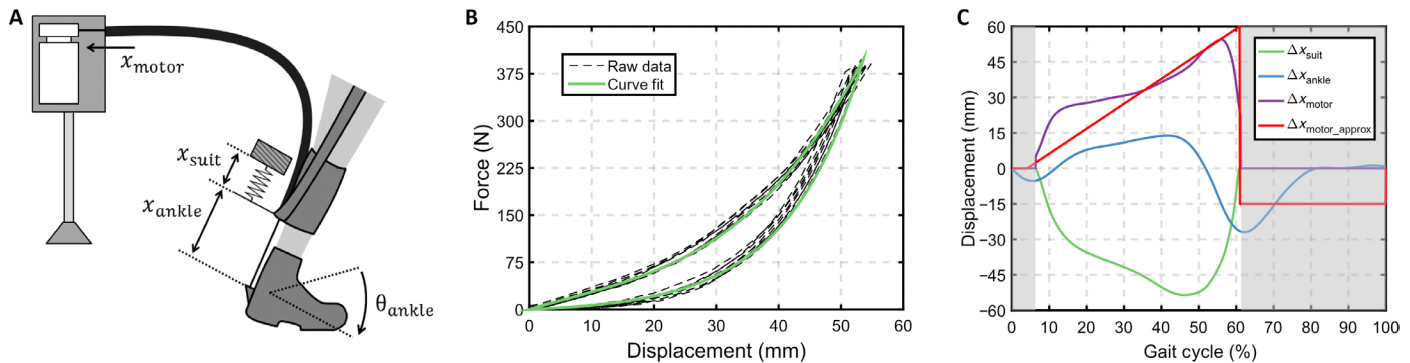
Fig. 6. Summary of biologically inspired controller. (A) Model of the system stiffness, where Δx_{motor} is the summation of (i) the travel required to track the ankle motion (Δx_{ankle}) and (ii) the travel due to the soft functional textile stretching and the human tissue compressing for a desired force profile (Δx_{suit}). **(B)** Static suit stiffness curve based on the Bowden cable position and force applied to the soft functional textile, as previously described by Asbeck *et al.* (*37*). **(C)** Values for Δx_{ankle} and Δx_{suit} across the gait cycle and the resulting calculation of Δx_{motor}, which was approximated as Δx_{motor_approx} for the controller developed in this study.

with the powered-off condition. At the hip, biological moment and positive power decreased significantly, most likely because of a combination of direct assistance applied to the hip and a transfer of energy between the hip and the ankle. At the ankle, the overall kinetic and kinematic joint behavior changed significantly, possibly as a result of the human attempting to optimize their energetics by acquiring more energy from the device. The results presented in this study have provided new insights into the human response to external assistance, in terms of both metabolic reduction and kinematic/kinetic adaptations, which may benefit future studies on design and control of assistive devices. Moreover, if combined with simple models of actuator power density and their associated metabolic burdens, such insights could move us one step further toward the design of a more optimal mobile exosuit.

MATERIALS AND METHODS
The aim of this study was to isolate and characterize the relationship between the exosuit assistance magnitude (i.e., peak exosuit ankle moment) and the metabolic cost of unloaded walking, with an understanding that the underlying mechanics of human locomotion may be used to understand changes in metabolic cost. To achieve this, we performed a series of experiments in which assistance with a multiarticular exosuit was varied over a wide range; peak assistive force applied to the textile architecture, local to the ankle, was scaled on the basis of each person's body weight: 18.7% (LOW), 37.5% (MED), 56.2% (HIGH), and 75.0% (MAX). While the participants walked on a treadmill, assistance was provided with an off-board actuation system to isolate the relationship between assistance and metabolic reduction, without the effect of system mass. In an attempt to deliver an assistive moment profile similar to the biological moment, we used a biologically inspired controller based on both the human kinematics and exosuit stiffness.

As for experimental design of the study, although seven people participated, no statistical methods were used to predetermine the sample size, and it was selected according to standard practice for locomotion research. The order of the experimental conditions was randomized, and details about the experimental procedure can be found in the "Experimental protocol" section. Each participant underwent each experimental condition once, and sampling was carried out for 10 strides for joint kinematics/kinetics and 2 min for metabolic rate to generate average data. Blinding was not applicable to this

study because both participants and conductors could immediately distinguish each condition during the experiment.
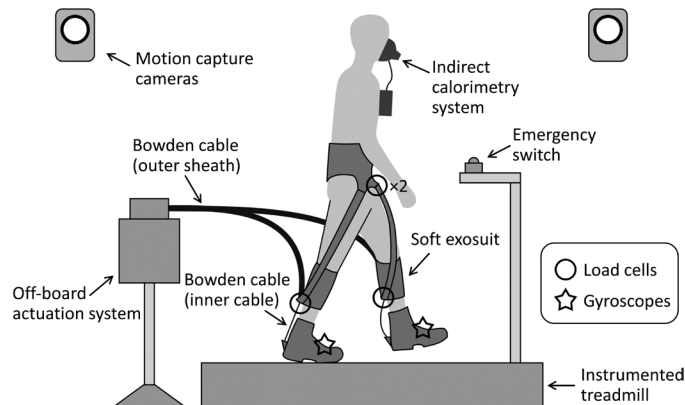
Soft exosuit
The multiarticular soft exosuit used in this study was designed to assist with both ankle plantar flexion and hip flexion while minimizing moments generated about the knee, as shown in Fig. 1 and previously described by Lee *et al.* (*21*). The exosuit consisted of a spandex base layer, a waist belt, two calf wraps, and four vertical straps (two per leg) crossing from the back of the calf wrap, through the center of the knee joint axis, to the front of the waist belt. All textile components (size medium) had a total mass of 0.89 kg. Of note, the ratio between the peak force applied at the ankle and the peak force applied at the hip was about 10:7 (fig. S7). More details on the soft exosuit design and the specific components can be found in figs. S1 to S4.

Actuation system and sensors
An off-board actuation system was used to generate assistive forces. It consisted of two actuators (EC 4-pole motors, Maxon Motor) and pulleys, and all components were as those described by Lee *et al.* (*21*) except that 80-mm-diameter pulleys were used. Bowden cables were used to transmit the forces from the actuator to the exosuit locally to the ankle joint. On the actuator side, the Bowden cable sheath connects to the outer frame of the pulley cover, and its inner cable attaches to the pulley. On the human side, the Bowden cable sheath connects to the back of the calf wrap and the bottom of the vertical straps, whereas its inner cable extends further to the metal bracket at the back of the heel of the boot. As the motor retracts, the distance between the two attachment points is shortened, generating a force that is distributed to both the calf wrap and the vertical straps.

One load cell (LTH300, FUTEK Advanced Sensor Technology) and one gyroscope (LY3100ALH, STMicroelectronics) per leg were attached to measure real-time data from the wearer and the exosuit. The load cell was placed in series with the Bowden cable and the calf wrap/vertical straps to measure the force delivered to the suit. The gyroscope was at the top of the midfoot to measure the angular motion of the foot for gait segmentation. To measure the assistive force transmitted to the hip joint, we added two additional load cells (LSB200, FUTEK Advanced Sensor Technology) to the left side of exosuit in series with the two vertical straps and the waist belt.

Fig. 7. Experimental setup. While a participant is walking with the soft exosuit, an off-board actuation system generates assistive forces and Bowden cables transfer the forces to the exosuit. Sensors (load cells and gyroscopes) are attached to measure real-time data. Body segment motions (motion capture), ground reaction forces (instrumented treadmill), and metabolic rate (indirect calorimetry) are measured.

Biologically inspired control

The exosuit control approach used in this study can be divided into two levels: (i) the high-level control design inspired by biomechanics of human walking and (ii) the low-level implementation of force-based position control.

(i) The high-level control profile was designed considering the force-displacement characterization of the human-exosuit system as well as the ankle kinematics and kinetics during human walking, similar to the robotic-tendon methodology proposed by Hollander *et al.* (*35*). This is not an actual implementation of a real-time controller but a design rationale of a specific assistance profile as a function of the gait cycle that is computed ahead of time and timed on the basis of our gait segmentation approach. As shown in Fig. 6, the desired motor position trajectory (Δx_{motor}) can be determined on the basis of the motion required to track the ankle displacement (Δx_{ankle}) and the motion required to produce a desired force profile for a given exosuit displacement (Δx_{suit}). Throughout the gait cycle, Δx_{ankle} (Fig. 6C, blue curve) can be estimated as $r*\theta_{\text{ankle}}$, where r is the moment arm toward the ankle joint center and θ_{ankle} is the ankle joint angle in radians. Here, r was approximated to be 10 cm on the basis of previous data analysis (*21*), and a typical ankle angle trajectory during normal walking (*36*) was used for θ_{ankle}. In addition, the static suit-human series stiffness was measured by applying force to a participant during standing, while collecting Bowden cable position using a motor encoder and force applied to the soft functional textile using a load cell, as previously described by Asbeck *et al.* (*37*). Given this suit-human series stiffness and a typical ankle moment (*36*), we can determine Δx_{suit} (green curve), the amount of cable travel that is required to stretch the soft functional textile and compress the human tissue to generate a desired percentage of ankle moment; for the example in Fig. 6C, we selected 25% of the ankle plantar flexion moment. Last, we can calculate the desired motor position trajectory as $\Delta x_{\text{motor}} = \Delta x_{\text{ankle}} + \Delta x_{\text{suit}}$ (purple curve). For this study, we approximated Δx_{motor} as a linear function ($\Delta x_{\text{motor\_approx}}$), which is depicted in Fig. 6C (red curve).

(ii) As an actual implementation of the designed control profile, the system performed a force-based position control of the cable on a step-by-step basis based on the given desired peak assistive force as in other work (*21*). The real-time gait cycle was segmented on the

basis of the heel strikes detected by the gyroscope on foot (*18*). Starting from the heel strike (0% of the gait cycle), the motor was controlled to retract the Bowden cable at a constant speed until the end of stance phase (about 60% of the gait cycle), following the linear motor position profile designed above (Fig. 6C, red curve). Immediately before the swing phase, the motor released the cable such that the system did not create undesired forces or hinder the wearer's natural motion. At the end of the gait cycle, the controller altered the maximum retraction length of the cable for the next step by comparing the given desired peak force and the actual peak force measured by the load cell during the step.

Experimental protocol

Seven healthy male adults (age, 26.7 ± 4.8 years; mass, 68.4 ± 9.5 kg; height, 1.7 ± 0.1 m; mean ± SD) participated in this study; no statistical methods were used to predetermine sample size, and it was selected according to standard practice for locomotion research. The study was approved by the Harvard Longwood Medical Area Institutional Review Board, and all methods were carried out in accordance with the approved study protocol. All participants provided written informed consent before their participation and after the nature and possible consequences of the studies were explained. All participants attended two experimental sessions: a training session and a testing session. In both sessions, participants walked on a treadmill at 1.50 m s^{-1} under five experimental conditions: one powered-off and four active. We chose to use a powered-off condition as opposed to a condition while walking without the exosuit to reduce the length of testing sessions and avoid repositioning the markers used for kinematic analysis, which could have led to increased variability.

During the four active conditions, peak assistive force applied at the ankle was scaled on the basis of each participant's body weight: 18.7% (LOW), 37.5% (MED), 56.2% (HIGH), and 75.0% (MAX). During the testing session, participants began with an 8-min warm-up period where they experienced all force magnitudes, and the initial motor position was set to keep the Bowden cables taut. After the warm up, the participants underwent the four experimental conditions, each 5 min in length; the order of the experimental conditions was randomized and grouped into two continuous trials, each containing a 5-min powered-off condition for relative comparison of metabolic data and, thus, each 15 min in length. A 5-min break was given between the 15-min continuous trials, and blinding was not applicable to this study because both participants and conductors could immediately distinguish each condition during the experiment. All energetics and biomechanics measurements were conducted in the testing session (Fig. 7).

Joint kinematics and kinetics

Body segment motions were measured using a reflective marker motion capture system (Vicon, Oxford Metrics; 120 Hz). Three-dimensional ground reaction forces were measured using an instrumented split-belt treadmill (Bertec; 2160 Hz). All markers and force trajectories were filtered using a zero-lag, fourth-order, low-pass Butterworth filter with an optimal cutoff frequency of 5 to 9 Hz that was selected using a custom residual analysis algorithm (MATLAB, MathWorks). Joint angles, total joint moments, and total joint powers were calculated for the right leg in the sagittal plane using kinematic and inverse dynamic analyses (Visual3D, C-Motion). Total joint moments and powers were then normalized by each participant's body mass. An automatic gait event detection algorithm (Visual3D, C-Motion)

was used to determine heel strikes that defined gait cycles. Ten strides per condition were used for generating mean kinematic and kinetic data for each participant, which were subsequently combined to calculate condition mean data.

To compute exosuit moment and power during the active conditions, we synchronized the data from the actuation units and suit-mounted sensors using motion capture data. The forces collected by the load cells at the ankle and the hip were segmented on the basis of the heel strike times obtained by the automatic gait events detection algorithm. Ankle exosuit moment was calculated for each participant, multiplying the force recorded by the load cells by the corresponding ankle moment arm. The ankle moment arm was calculated using the perpendicular distance between the joint center and line between markers on either end of the exposed inner Bowden cable (boot attachment and calf wrap). Hip flexion moments were calculated as the summation of the exosuit moments from both vertical straps (medial and lateral). Both strap moments were calculated by multiplying the force from the load cell in that strap by the moment arm calculated from that strap (perpendicular distance between the hip joint center and the line between two markers on the vertical straps).

Biological moments were calculated as the difference between the total and exosuit moment at each joint. Biological powers were calculated as the difference between total and exosuit power.

Metabolic rate

Metabolic rate during walking was assessed by means of indirect calorimetry (K4b2, Cosmed), which enabled the measurement of expired gas concentrations and volumes. Further, carbon dioxide and oxygen rate were averaged across the last 2 min of each condition and used to calculate metabolic power using a modified Brockway equation (38). Net metabolic rate for each condition of testing was obtained by subtracting the metabolic rate obtained during a standing trial performed at the beginning of each data collection session, the average of which was 1.464 ± 0.380 W kg^{-1}, from the metabolic power calculated during the walking conditions. Last, the net metabolic reduction was calculated by taking the difference in net metabolic rates between each active condition and the powered-off condition that was recorded within the same 15-min bout of walking. Multiple powered-off conditions (one in each 15-min bout) were used to account for changes in baseline metabolics over time (39). All net metabolic rates and reductions were normalized to participant's body mass.

Note that the changes in net metabolic rate were calculated relative to a powered-off condition and not a no-suit condition; thus, the effect of just wearing the suit components is incorporated into the metabolic results. This was done to simplify the protocol and reduce the time between relative metabolic comparisons such that participants did not have to stop and doff the suit between conditions. It is currently unknown how such a comparison would change the results, but due to the lightweight nature of the suit components (0.89 kg), we expect that the difference would be negligible. For this reason, the augmentation factor proposed by Mooney *et al.* (40) was not calculated in this study because of the lack of a strict no-suit condition.

Statistics

For each condition, means and interparticipant SEs were calculated for the net metabolic reduction, peak moments during push-off, average positive and negative powers, and peak flexion/extension angles. On all outcome measures, we conducted a mixed-model, two-factor

ANOVA (random effect: participant; fixed effects: peak exosuit ankle moment) to test for an effect of exosuit assistance across conditions (significance level $\alpha = 0.05$; MATLAB, MathWorks). For metabolic rate, we also used paired two-sided *t* tests with a Sidak-Holm correction (41) for multiple comparisons to compare the different active conditions with the powered-off condition to identify which exosuit ankle moment magnitudes exacted a significant change in metabolic rate. We also calculated the coefficient of determination of metabolics versus peak force.

SUPPLEMENTARY MATERIALS

robotics.sciencemag.org/cgi/content/full/2/2/eaah4416/DC1
Supplementary Text
Fig. S1. Structure of the waist belt component.
Fig. S2. Structure of the calf wrap component.
Fig. S3. Structure of the Y-strap part of the calf wrap component.
Fig. S4. Structure of the vertical strap component.
Fig. S5. Changes in ground reaction forces and center of mass velocity.
Fig. S6. Changes in center of mass power.
Fig. S7. Hip and ankle force profiles.
Fig. S8. Changes in biological joint moment.
Fig. S9. Changes in biological joint power.
Fig. S10. Net biological joint power.
Table S1. Changes in net metabolic rate for each participant.
Movie S1. Varying assistance level with a soft exosuit: Methods and metabolic results.
References (42–44)

REFERENCES AND NOTES

1. M. Y. Zarrugh, F. N. Todd, H. J. Ralston, Optimization of energy expenditure during level walking. *Eur. J. Appl. Physiol. Occup. Physiol.* **33**, 293–306 (1974).
2. S. H. Collins, P. G. Adamczyk, A. D. Kuo, Dynamic arm swinging in human walking. *Proc. Biol. Sci.* **276**, 3679–3688 (2009).
3. R. L. Waters, S. Mulroy, The energy expenditure of normal and pathologic gait. *Gait Posture* **9**, 207–231 (1999).
4. S. Agarwal, A. Z. Abidin, S. Chattopadhyay, U. R. Acharya, Engineering interventions to improve impaired gait, in *Advances in Therapeutic Engineering*, W. Yu, S. Chattopadhyay, T.-C. Lim, U. R. Acharya, Eds. (CRC Press, 2012).
5. G. Stoquart, C. Detrembleur, T. M. Lejeune, The reasons why stroke patients expend so much energy to walk slowly. *Gait Posture* **36**, 409–413 (2012).
6. C. L. Christiansen, M. L. Schenkman, K. McFann, P. Wolfe, W. M. Kohrt, Walking economy in people with Parkinson's disease. *Mov. Disord.* **24**, 1481–1487 (2009).
7. A. van den Hecke, C. Malghem, A. Renders, C. Detrembleur, S. Palumbo, T. M. Lejeune, Mechanical work, energetic cost, and gait efficiency in children with cerebral palsy. *J. Pediatr. Orthop.* **27**, 643–647 (2007).
8. J. Kang, E. C. Chaloupka, A. M. Mastrangelo, J. R. Hoffman, Physiological and biomechanical analysis of treadmill walking up various gradients in men and women. *Eur. J. Appl. Physiol.* **86**, 503–508 (2002).
9. J. J. Knapik, K. L. Reynolds, E. Harman, Soldier load carriage: Historical, physiological, biomechanical, and medical aspects. *Mil. Med.* **169**, 45–56 (2004).
10. K. N. Gregorczyk, J. P. Obusek, L. Hasselquist, J. M. S. Bensel, K. Carolyn, D. Gutekunst, P. Frykman, The effects of a lower body exoskeleton load carriage assistive device on oxygen consumption and kinematics during walking with loads, in *25th Army Science Conference*, Orlando, FL, 27 to 30 November 2006, pp. 1515–1529.
11. C. J. Walsh, K. Endo, H. Herr, A quasi-passive leg exoskeleton for load-carrying augmentation. *Int. J. Hum. Robot.* **4**, 487–506 (2007).
12. A. Schiele, Ergonomics of exoskeletons: Objective performance metrics, in *Proceedings of the Third Joint Eurohaptics Conference and Symposium Haptic Interfaces for Virtual Environment and Teleoperator Systems*, Salt Lake City, UT, 10 to 15 October 2009 [Institute of Electrical and Electronics Engineers (IEEE), 2009], pp. 103–108.
13. S. H. Collins, M. B. Wiggin, G. S. Sawicki, Reducing the energy cost of human walking using an unpowered exoskeleton. *Nature* **522**, 212–215 (2015).
14. P. Malcolm, W. Derave, S. Galle, D. De Clercq, A simple exoskeleton that assists plantarflexion can reduce the metabolic cost of human walking. *PLOS ONE* **8**, e56137 (2013).
15. G. S. Sawicki, D. P. Ferris, Mechanics and energetics of level walking with powered ankle exoskeletons. *J. Exp. Biol.* **211**, 1402–1413 (2008).
16. J. R. Koller, D. A. Jacobs, D. P. Ferris, C. D. Remy, Learning to walk with an adaptive gain proportional myoelectric controller for a robotic ankle exoskeleton. *J. Neuroeng. Rehabil.* **12**, 97 (2015).

17. L. M. Mooney, H. M. Herr, Biomechanical walking mechanisms underlying the metabolic reduction caused by an autonomous exoskeleton. *J. Neuroeng. Rehabil.* **13**, 4 (2016).

18. A. T. Asbeck, K. Schmidt, I. Galiana, D. Wagner, C. J. Walsh, Multi-joint soft exosuit for gait assistance, in *Proceedings of the 32nd IEEE International Conference on Robotics and Automation*, Seattle, WA, 26 to 30 May 2015 (IEEE, 2015), pp. 6197–6204.

19. Y. Ding, I. Galiana, A. Asbeck, S. De Rossi, J. Bae, T. Santos, V. Araujo, S. Lee, K. Holt, C.Walsh, Biomechanical and physiological evaluation of multi-joint assistance with soft exosuits. *IEEE Trans. Neural Syst. Rehabil. Eng.* (2016).

20. F. A. Panizzolo, I. Galiana, A. T. Asbeck, C. Siviy, K. Schmidt, K. G. Holt, C. J. Walsh, A biologically-inspired multi-joint soft exosuit that can reduce the energy cost of loaded walking. *J. Neuroeng. Rehabil.* **13**, 43 (2016).

21. S. Lee, S. Crea, P. Malcolm, I. Galiana, A. Asbeck, C. Walsh, Controlling negative and positive power at the ankle with a soft exosuit, *in Proceedings of the 33rd IEEE International Conference on Robotics and Automation*, Stockholm, 16 to 21 May 2016 (IEEE, 2016), pp. 3509–3515.

22. J. M. Caputo, S. H. Collins, Prosthetic ankle push-off work reduces metabolic rate but not collision work in non-amputee walking. *Sci. Rep.* **4**, 7213 (2014).

23. R. W. Jackson, S. H. Collins, An experimental comparison of the relative benefits of work and torque assistance in ankle exoskeletons. *J. Appl. Physiol.* **119**, 541–557 (2015).

24. C. L. Lewis, D. Ferris, Walking with increased ankle pushoff decreases hip muscle moments. *J. Biomech.* **41**, 2082–2089 (2008).

25. K. Seo, J. Lee, Y. Lee, T. Ha, Y. Shim, Fully autonomous hip exoskeleton saves metabolic cost of walking, in *Proceedings of the 33rd IEEE International Conference on Robotics and Automation*, Stockholm, 16 to 21 May 2016 (IEEE, 2016), pp. 4628–4635.

26. A. J. van den Bogert, Exotendons for assistance of human locomotion. *Biomed. Eng. Online* **2**, 17 (2003).

27. J. C. Selinger, S. M. O'Connor, J. D. Wong, J. M. Donelan, Humans can continuously optimize energetic cost during walking. *Curr. Biol.* **25**, 2452–2456 (2015).

28. M. Ishikawa, P. V. Komi, M. J. Grey, V. Lepola, G. P. Bruggemann, Muscle-tendon interaction and elastic energy usage in human walking. *J. Appl. Physiol.* **99**, 603–608 (2005).

29. G. S. Sawicki, C. L. Lewis, D. P. Ferris, It pays to have a spring in your step. *Exerc. Sport Sci. Rev.* **37**, 130–138 (2009).

30. D. J. Farris, B. D. Robertson, G. S. Sawicki, Elastic ankle exoskeletons reduce soleus muscle force but not work in human hopping. *J. Appl. Physiol.* **115**, 579–585 (2013).

31. D. J. Farris, J. L. Hicks, S. L. Delp, G. S. Sawicki, Musculoskeletal modelling deconstructs the paradoxical effects of elastic ankle exoskeletons on plantar-flexor mechanics and energetics during hopping. *J. Exp. Biol.* **217**, 4018–4028 (2014).

32. R. W. Jackson, C. L. Dembia, S. L. Delp, S. H. Collins, Estimated changes in muscle-level dynamics and energetics under different levels of exoskeleton-applied work and torque, abstr. no. 51, presented at the 12th Dynamic Walking Conference, Columbus, OH, 21 to 24 July 2015; available online at http://biomechatronics.cit.cmu.edu/publications/Jackson_2015_DW.pdf.

33. G. S. Sawicki, N. S. Khan, A simple model to estimate plantarflexor muscle-tendon mechanics and energetics during walking with elastic ankle exoskeletons. *IEEE Trans. Biomed. Eng.* **63**, 914–923 (2016).

34. N. Karavas, J. Kim, I. Galiana, Y. Ding, A. Couture, D. Wagner, A. Eckert-Erdheim, C. Walsh, Autonomous soft exosuit for hip extension assistance, in *Proceedings of the 2nd International Symposium Wearable Robotics*, Segovia, 18 to 21 October 2016 (Springer, 2016), pp. 331–335.

35. K. W. Hollander, R. Ilg, T. G. Sugar, D. Herring, An efficient robotic tendon for gait assistance. *J. Biomech. Eng.* **128**, 788–791 (2006).

36. D. A. Winter, *The Biomechanics and Motor Control of Human Gait: Normal, Elderly and Pathological* (Waterloo Biomechanics, 1991).

37. A. T. Asbeck, S. M. M. De Rossi, K. G. Holt, C. J. Walsh, A biologically inspired soft exosuit for walking assistance. *Int. J. Robot. Res.* **34**, 744–762 (2015).

38. J. M. Brockway, Derivation of formulae used to calculate energy expenditure in man. *Hum. Nutr. Clin. Nutr.* **41**, 463–471 (1987).

39. G. H. Markovitz, J. W. Sayre, T. W. Storer, C. B. Cooper, On issues of confidence in determining the time constant for oxygen uptake kinetics. *Br. J. Sports Med.* **38**, 553–560 (2004).

40. L. M. Mooney, E. J. Rouse, H. M. Herr, Autonomous exoskeleton reduces metabolic cost of human walking during load carriage. *J. Neuroeng. Rehabil.* **11**, 80 (2014).

41. S. A. Glantz, *Primer of Biostatistics* (McGraw-Hill Medical, 2005).

42. J. M. Donelan, R. Kram, A. D. Kuo, Simultaneous positive and negative external work in human walking. *J. Biomech.* **35**, 117–124 (2002).

43. R. C. Browning, J. R. Modica, R. Kram, A. Goswami, The effects of adding mass to the legs on the energetics and biomechanics of walking. *Med. Sci. Sports Exerc.* **39**, 515–525 (2007).

44. Y. Ding, F. A. Panizzolo, C. Siviy, P. Malcolm, I. Galiana, K. G. Holt, C. J. Walsh, Effect of timing of hip extension assistance during loaded walking with a soft exosuit. *J. Neuroeng. Rehabil.* **13**, 87 (2016).

Citation: B. T. Quinlivan, S. Lee, P. Malcolm, D. M. Rossi, M. Grimmer, C. Siviy, N. Karavas, D. Wagner, A. Asbeck, I. Galiana, C. J. Walsh, Assistance magnitude versus metabolic cost reductions for a tethered multiarticular soft exosuit. *Sci. Robot.* **2**, eaah4416 (2017).